tvst

Glaucoma

AAV2-Mediated Expression of HspB1 in RGCs Prevents Somal Damage and Axonal Transport Deficits in a Mouse Model of Ocular Hypertension

Mi-Hyun Nam[1], Rooban B. Nahomi[1], Mina B. Pantcheva[1], Armaan Dhillon[1], Vince A. Chiodo[2], W. Clay Smith[2], and Ram H. Nagaraj[1,3]

[1] Sue Anschutz-Rodgers Eye Center and Department of Ophthalmology, School of Medicine, University of Colorado, Anschutz Medical Campus, Aurora, CO, USA
[2] Department of Ophthalmology, University of Florida, Gainesville, FL, USA
[3] Department of Pharmaceutical Sciences, Skaggs School of Pharmacy and Pharmaceutical Sciences, University of Colorado, Anschutz Medical Campus, Aurora, CO, USA

Correspondence: Mi-Hyun Nam and Ram H. Nagaraj, Department of Ophthalmology, University of Colorado, School of Medicine, 12800 East 19th Avenue, RC-1 North, 5102, Aurora, CO 80045, USA. e-mails: mi-hyun.nam@cuanschutz.edu, ram.nagaraj@cuanschutz.edu.

Received: April 14, 2022
Accepted: October 2, 2022
Published: November 10, 2022

Keywords: glaucoma; ocular hypertension; retinal ganglion cells; gene therapy; HspB1

Citation: Nam MH, Nahomi RB, Pantcheva MB, Dhillon A, Chiodo VA, Smith WC, Nagaraj RH. AAV2-mediated expression of HspB1 in RGCs prevents somal damage and axonal transport deficits in a mouse model of ocular hypertension. Transl Vis Sci Technol. 2022;11(11):8, https://doi.org/10.1167/tvst.11.11.8

Purpose: Ocular hypertension is a significant risk factor for vision loss in glaucoma caused by the death of retinal ganglion cells (RGCs). We investigated whether small heat shock proteins (sHsps) expressed in RGCs protect those cells against ocular hypertension in mice.

Methods: AAV2 vectors encoding genes for one of the following four human sHsps: *HSPB1, HSPB4, HSPB5,* or *HSPB6* were constructed for RGC-specific expression. Ischemia/reperfusion was induced by elevating the intraocular pressure (IOP) to 120 mm Hg for one hour, followed by a rapid return to normal IOP. Microbeads (MB) were injected into the anterior chamber of mice to induce ocular hypertension. RGC death and glial activation were assessed by immunostaining for Brn3a, RBPMS, Iba1, and glial fibrillary acid protein in retinal flat mounts. RGC axonal defects were evaluated by anterograde transport of intravitreally injected cholera toxin-B. RGC function was assessed by pattern electroretinography.

Results: Among the sHsps, HspB1 offered the best protection against RGC death from ischemia/reperfusion injury in the mouse retina. Intravitreal administration of AAV2-*HSPB1* either two weeks before or one week after instituting ocular hypertension resulted in significant prevention of RGC loss. The MB-injected mice showed RGC axonal transportation defects, but AAV2-*HSPB1* administration significantly inhibited this defect. AAV2-*HSPB1* prevented glial activation caused by ocular hypertension. More importantly, a single injection of AAV2-*HSPB1* protected RGCs long-term in MB-injected eyes.

Conclusions: The administration of AAV2-*HSPB1* inhibited RGC death and axonal transport defects and reduced glial activation in a mouse model of ocular hypertension.

Translational Relevance: Our results suggested that the intravitreal delivery of AAV2-*HSPB1* could be developed as a gene therapy to prevent vision loss on a long-term basis in glaucoma patients.

Introduction

Glaucoma is a progressive neurodegenerative disease characterized by the death of retinal ganglion cells (RGCs) and degeneration of the optic nerve. Globally, more than 75 million people are affected by this disease, and this number is expected to increase to approximately 110 million by 2040.[1] Elevated intraocular pressure (IOP) is a significant risk factor for RGC death along with other risk factors, including age, race, and genetics.[2] IOP-lowering drugs, and

surgical techniques to decrease IOP have shown beneficial effects in saving vision in glaucoma patients.[3] However, approximately 10% of glaucoma patients do not respond to these treatments and show continued deterioration of vision through the loss of RGCs.[3,4] Thus there is an urgent unmet medical need to develop efficacious and long-lasting therapies to prevent RGC death in glaucoma.

Previous studies have shown the involvement of multiple factors, such as inflammation, oxidative stress, deprivation of neurotrophic factors, dysfunction of mitochondria, damage caused by excitotoxicity, and axonal transport failure, in the pathogenesis of glaucoma.[5–8] However, the fundamental biological processes that lead to RGC death are still poorly understood. Prevention of RGC death in animal models has been a focus of research for many years, with several small molecules and biologics being tested.[9–13] However, a significant limitation in several of these studies is the failure to protect the soma and axons of RGCs simultaneously. Therefore new therapeutics that protect both the RGC soma and axons are needed to prevent vision loss in glaucoma.

Small heat shock proteins (sHsps) are a family of stress response proteins that are molecular chaperones possessing anti-apoptotic properties. There are 11 members in this family, and all have a highly conserved "α-crystallin" core domain (except for Hsp11).[14–16] SHsps bind to structurally perturbed proteins in an adenosine triphosphate (ATP)-independent manner and inhibit protein denaturation and aggregation. In addition, they inhibit stress-mediated apoptosis by blocking both the extrinsic and intrinsic pathways of apoptosis[17] while also possessing antioxidant and anti-inflammatory properties.[18–20]

Previous studies have shown changes in sHsp levels in experimental glaucoma models. We found lower levels of HspB5 in glaucomatous than in nonglaucomatous human retinas.[21] We also observed lower RGC numbers in *CRYAB* knockout mouse retinas than in wild-type mouse retinas.[21] Ocular hypertension-induced RGC degeneration in rats was accompanied by suppression of the mRNA expression and protein levels of HspB4 and HspB5.[22,23] In addition, reduced HspB4 levels were observed in the retinas of glucocorticoid-induced ocular hypertensive rats compared to controls.[24] Furthermore, in a mouse genetic model for glaucoma (DBA/2J mouse), crystallin gene expression in the retina was downregulated.[25] Studies have shown that exogenous delivery of HspB5 into the vitreous protects RGCs in several animal models of glaucoma. Intravitreally administered HspB5 reduced axonal injury and RGC death because of IOP elevation in mice.[26,27] In optic nerve injury models, intravenous injection of HspB5 reduced microglial activation and increased RGC survival,[28] and transfection of HspB4 and HspB5 into the vitreous followed by electroporation showed an increase in the number of surviving RGCs.[29] Our previous study demonstrated that the chaperone peptide of HspB5 (peptain-1) injected intraperitoneally inhibited RGC loss in mouse retinas subjected to ischemia/reperfusion (I/R) injury and in a Morrison rat model of glaucoma.[21]

Although the beneficial effects of HspB5 on RGCs are evident, the effects of HspB1 are ambiguous. Elevation of IOP through laser photocoagulation of the episcleral and limbal veins resulted in elevated expression of HspB1 in RGCs of rats.[30] Additional studies have shown elevated expression of HspB1 in RGCs under stressful conditions that are permissive for RGC death.[31–33] These observations imply that RGCs express higher levels of HspB1 as a protective mechanism. In support of this notion is the observation that electrophoretically delivered HspB1 into RGCs protects those cells against retinal I/R injury in rats.[34] However, recent studies suggest that exogenous delivery of HspB1 into the vitreous could be detrimental to RGCs; it has been observed that intravitreal injection of HspB1 led to the death of RGCs in rats[35] via activation of caspases.[36] Furthermore, in microbeads (MB)-induced ocular hypertension in mice, a T-cell–specific response to HspB1 was implicated as a cause of RGC death.[37] A direct correlation between axonal regeneration in neurons and the expression of HspB1 was also observed.[38] Although supplementation with bacterial-expressed human HspB1 in the vitreous was detrimental to RGCs, intracellular expression of HspB1 in RGCs protected these cells from I/R injury. These seemingly contrasting observations led us to test the hypothesis that intracellular but not extracellular elevation of HspB1 protects RGCs in animal models of glaucoma.

AAV2 has excellent tropism[39–41]; it is relatively safe, efficacious, and approved by the Food and Drug Administration to treat Leber congenital amaurosis through the expression of RPE65 in retinal pigment epithelial cells.[42] In this study, we report the protection of RGCs in an ocular hypertension mouse model through adeno-associated viral vector serotype 2 (AAV2)–mediated expression of HspB1 specifically in RGCs.

Methods

Construction of AAV-2 Vectors Expressing sHsps

We obtained AAV2 vectors encoding human HspB1, HspB4, HspB5, or HspB6 with a mini RGC-specific promoter Ple345 (neurofilament, light polypeptide, *NEFL*) for specific expression in RGCs (Ocular Gene Therapy Core, University of Florida Health Science Center, Gainesville, FL, USA). The mini Ple345 promoter is highly efficient in targeting RGCs.[43] All vectors were packaged and purified by standard methods as previously described,[44,45] and aliquots were stored at −80°C and thawed no more than two times before use.

Animals

All animal experiments were reviewed and approved by the University of Colorado Denver Institutional Animal Care and Use Committee and performed under adherence to the ARVO Statement for the Use of Animals in Ophthalmic and Vision Research. C57BL/6J mice were obtained from Jackson Laboratories (Stock No: 000664, Bar Harbor, ME, USA) or bred in-house with a 12:12-h light/dark cycle with access to food and water as desired. This study included both male and female mice.

Transduction of sHsps

Eight- to twelve-week-old mice were anesthetized with an intraperitoneal injection of ketamine/xylazine. Their eyes were anesthetized with topical 0.5% proparacaine hydrochloride ophthalmic solution (Akorn, Somerset, NJ, USA). Appropriate anesthesia was confirmed by the toe-pinch pain test. The animals were then placed on a heating pad to maintain their body temperature throughout the procedure. A puncture through the sclera of the right eye was made approximately 0.5 mm posterior to the limbus with a 33 G needle and observed under a dissecting microscope. One microliter of vector (1×10^9 viral genomes in 1 µL of HBSS) was slowly injected through this aperture using a blunt 34G needle connected to a 5 µL Hamilton syringe, and the needle was kept inside the eye for 30 seconds. For each AAV2-sHsp treatment, we had five mice (three for retinal sections and two for Western blotting). After four weeks, the transduction of sHsps was assessed in retinal sections by immunofluorescence and in retinal homogenates by Western blotting.

For the retinal sections, eyes were fixed in 4% PFA overnight. The retinas were incubated in 10%, 20%, and 30% sucrose and embedded in Tissue Tek OCT compound (Sakura Finetek, Torrance, CA, USA) before rapid freezing. Retinal sections (12 µm thickness) were cryosectioned, blocked for one hour, immunolabeled with primary antibodies (1:50 dilution) overnight at 4°C, and incubated with secondary antibodies (1:250) for two hours at room temperature. The primary antibodies were as follows: HspB1 (Cat no. 2402S; Cell Signaling Technology, Danvers, MA, USA), HspB4 (Cat no. ADI-SPA-221; Enzo Life Sciences, Farmingdale, NY, USA), HspB5 (Cat no. ABN185; Millipore, Billerica, MA, USA), and HspB6 (Cat no. ADI-SPA-796, Enzo Life Sciences).

Retinal homogenates were prepared in 150 µl of 1X RIPA buffer (Thermo, Cat no. 89900) containing a protease inhibitor cocktail (1:100; Sigma-Aldrich Corp., St. Louis, MO, USA) by a hand-held homogenizer. Western blotting was performed as previously described.[46] The sHsp-specific primary antibodies (1:1,000 dilution) were incubated overnight at 4°C. Anti-rabbit IgG (1:5,000 dilution, Cat no. 7074; Cell Signaling Technology, Inc., Beverly, MA, USA) or anti-mouse IgG (1:5,000 dilution, Cat no. 7076; Cell Signaling Technology, Inc.) secondary antibodies were incubated at room temperature for one hour. The protein bands were visualized with the SuperSignal West Pico Kit (Pierce Chemicals, Rockford, IL, USA). GAPDH was used as a loading control.

Retinal I/R Injury

After four weeks of AAV2 injection, the right eye of each mouse was cannulated into the anterior chamber with a 33 gauge needle connected to an elevated saline solution (0.9% NaCl) reservoir. The height of the reservoir was adjusted to achieve an intraocular pressure of approximately 120 mm Hg. After 60 minutes of elevated pressure, the needle was removed. For each AAV2-sHsp treatment, we had five to seven mice. The animals were euthanized on day 14 post I/R injury. The contralateral uninjured eyes from the vehicle group were used as control.

MB-Induced Ocular Hypertensive Mouse Model

Ocular hypertension was induced by injection of polystyrene MB (FluoSpheres; Invitrogen, Carlsbad, CA, USA; 10 µm diameter) into the anterior chamber of the right eye of each animal. MB was reformulated at a concentration of 5×10^7 beads/mL

in phosphate-buffered saline solution (PBS). The pupil was dilated with one drop of a phenylephrine hydrochloride/tropicamide (4:1) mixture. The cornea was gently punctured near the center using a 33G needle, and a small air bubble was injected to raise the anterior chamber. Two microliters of MB were injected into the anterior chamber under the bubble via a blunt 33G needle connected to a Hamilton. An antibiotic ointment was applied topically onto the injected eye to prevent infection. The IOP was monitored weekly until 20 weeks using a TonoLab tonometer (Colonial Medical Supply, Espoo, Finland).

To study the prophylactic effects of AAV2-*HSPB1,* we used 29 mice (seven treated with vehicle, 10 treated with AAV2 control, and 12 treated with AAV2-*HSPB1*), which were euthanized at four weeks post MB injection (WPI). To study the therapeutic effects AAV2-*HSPB1,* we used 79 mice (13 treated with vehicle, 34 treated with AAV2 control, and 32 treated with AAV2-*HSPB1*), which were euthanized at one, two, four, and six WPI (n = 4–9 in each category). Twelve mice that received MB injection followed by AAV2 control or AAV2-*HSPB1* injection (n = 6 in each category) were euthanized at 20 WPI. Mice were considered to have ocular hypertension when the IOP was ≥ 16 mm Hg after one week of MB injection. Twelve mice that did not show elevated IOP after MB injection or showed signs of anterior segment inflammation or vitreous hemorrhage were excluded from the study.

Tissue Processing and Immunohistochemistry

After four to five weeks of MB injection, the eyes were fixed with 4% paraformaldehyde (Cat no. 15710; Electron Microscopy Sciences, Hatfield, PA, USA) overnight at 4°C. The next day, the fixative solution was aspirated, and the retinas were dissected out, rinsed, and permeabilized with PBS containing 0.1% sodium citrate and 0.2% Triton-X100 for five minutes. Retinas were blocked in 5% normal donkey serum (Cat no. 017-000-121, Jackson ImmunoResearch Labs Inc., West Grove, PA, USA) and 1% Triton X-100 in PBS overnight. To count surviving RGCs, whole-mount retinas were immunostained with Brn3a antibody (1:500 dilution, Cat# MAB1585, EMD Millipore, Bedford, MA) and/or RBPMS antibody (1:500 dilution, Cat no. GTX118619; GeneTex, Irvine, CA, USA) for three days at 4°C followed by Alexa Fluor 488 donkey anti-mouse or Texas red-conjugated goat anti-rabbit IgG (1:250 dilution; Invitrogen, Carlsbad, CA, USA) overnight at 4°C. To determine glial activation, retinas were stained for the microglial activation marker Iba1 (ionized calcium-binding adaptor molecule 1, 1:500 dilution, Cat no. ab178846; Abcam, Cambridge, MA, USA) and the astrocyte activation marker glial fibrillary acid protein (GFAP; 1:500 dilution, Cat no. 12389; Cell Signaling Technology) for two days at 4°C followed by Alexa Fluor 647 donkey anti-rabbit IgG (1:250 dilution; Jackson ImmunoResearch Labs) overnight at 4°C. Using a sharp scalpel blade, the retinas were cut into four petal shapes for flat mounts and mounted with Vectashield mounting medium (H-1200). Four fields from each mid-peripheral retina were taken using an objective lens ×20 with a Zeiss confocal microscope (Nikon Eclipse Ti; Nikon Instruments Inc., Tokyo, Japan). The percentage of RGC survival was calculated as the ratio of surviving RGC numbers (cells/mm^2) in injured eyes compared to contralateral uninjured eyes.

Axonal Transportation

CT-B is an established neuronal tracer used to assess retinal projection to the brain.[47] To assess anterograde axonal transport, the mice were anesthetized with ketamine/xylazine and intravitreally injected with 1 µL of 0.2% CT-B (Alexa Fluor 555 Conjugate; Thermo Fisher, , St. Louis, MO, USA; Cat no. C22843). After the injection, the needle was slowly withdrawn, and the injected area was treated with an antibiotic ointment. The next day, the mice were sacrificed, and the optic nerves were dissected, fixed in 4% PFA overnight, and dehydrated in methanol for five minutes. The optic nerves were cleared by incubation with Visikol HISTO-1 for one week, transferred to Visikol HISTO-2 and incubated for an additional week. Optic nerves were mounted in Visikol HISTO-2 solution and imaged using an objective lens ×10 with confocal microscopy. The mean fluorescence intensities were analyzed using ImageJ software (NIH).

Pattern Electroretinography (pERG)

To assess RGC function, pERG was performed using the pERGsystem (Jorvec, Inc., Miami, FL, USA) as previously described.[48] Briefly, the mice were anesthetized with ketamine/xylazine. After that, a drop of GenTeal gel (Alcon Laboratories, Fort Worth, TX, USA) was applied to the cornea, and body temperature was maintained at 37°C using a thermal pad. To acquire pERG responses, a needle electrode (Intelligent Hearing Systems, Miami, FL, USA) was inserted subdermally on the snout. The reference electrode was inserted on the back of the head, and the ground electrode was placed at the base of the tail. The

center of the display monitors was positioned 10 cm from each eye. The pattern consisted of four cycles of the white elements at maximum luminance and the black elements at minimum luminance. For each eye, 372 traces were recorded, the average waveform was calculated, and the amplitude (μV) from the first positive peak (P1) to the second negative peak (N2) was measured.

Statistical Analysis

GraphPad Prism software version 9 (GraphPad Prism Software, Inc., San Diego, CA, USA) was used for statistical analyses. We used one-way analysis of variance and multicomparison tests to determine the significance of differences among the animal groups. A P value < 0.05 was considered statistically significant.

Results

Transduction of AAV-2-Delivered sHsps in Retinal RGCs

We used an RGC-specific neurofilament light chain promoter (Ple345) to drive the expression of sHsps in RGCs (Supplementary Fig. S1).[43] Figure 1A shows retinal sections immunostained for sHsps. Intravitreally delivered AAV2-sHsps resulted in extensive transduction of sHsps in RGCs after four weeks. In parallel, Western blots of retinal homogenates showed robust expression of sHsps (Fig. 1B).

AAV2-*HSPB1* Protects RGCs From I/R Injury in Mice

To determine which sHsp is the most protective against RGC death in the retina, we first tested them in mice with retinal I/R injury. We intravitreally delivered AAV2-sHsps and, after four weeks, induced I/R injury. Two weeks post-I/R injury, the retinas were dissected, flat mounted and immunostained for RGC marker, brain-specific homeobox/POU domain protein 3A (Brn3a). We observed non-specific staining for mouse IgGs in blood vessels. Mice receiving vehicle alone after I/R injury showed a 57% loss of Brn3a +ve RGCs in the mid-peripheral retina relative to uninjured retinas ($P < 0.0001$, Figs. 1C, 1D). However, with prior AAV2-sHsp administration, the RGC losses were 44%, 33%, 19%, and 11% with AAV2-*HSPB4*, AAV2-*HSPB5*, AAV2-*HSPB6,* and AAV2-*HSPB1*, respectively. When compared to the vehicle-treated eyes, these values were significantly different for AAV2-*HSPB6* ($P < 0.05$) and AAV2-*HSPB1* ($P < 0.01$). Among the four AAV2-sHsps tested, AAV2-*HSPB1* was the most efficient in protecting RGCs and was selected for further testing.

Because a previous study showed that intravitreal HspB1 injection leads to RGC loss in rats within three weeks,[35] we first assessed whether RGC-specific expression of HspB1 causes retinal damage. Hematoxylin and eosin staining of sections of the ocular globes six weeks after AAV2-*HSPB1* injection (1 and 5 × 10^9 vg/retina) had no adverse effects on retinal morphology. In addition, we measured RBPMS +ve RGC numbers in the retinal cross-sections of AAV2-*HSPB1*-injected eyes. The RGC numbers were similar between AAV2-*HSPB1* and uninjured contralateral eyes (Supplementary Fig. S2).

Prophylactic Effects of AAV2-*HSPB1* in a Mouse Model of Glaucoma

The pathogenesis of glaucoma is not well understood, but elevated IOP is a significant risk factor for RGC death and axonal damage.[49,50] Thus we determined whether AAV2-*HSPB1* protects RGCs against ocular hypertension. We injected 2 μL of MB into the anterior chamber of the right eye of mice to reduce the aqueous outflow and elevate the IOP.[51] We injected AAV2-*HSPB1* (1-5 × 10^{12} vg/mL) or AAV2-control (1 × 10^{12} vg/mL) into the vitreous one week before injecting MB (Fig. 2A). The baseline IOP was ∼10 mm Hg, it was significantly ($P < 0.0001$) elevated after one week of MB injection and then gradually declined over the following four-week period but remained significantly ($P < 0.001$) elevated over control eyes (Fig. 2B). We assessed the expression of HspB1 in whole retinal flat mounts. The injection of AAV2-*HSPB1* did not change the number of RBPMS +ve RGCs compared to the uninjured contralateral eyes (Supplementary Fig. S3A). Based on the immunofluorescence intensity, AAV2-*HSPB1* injection robustly increased the levels of HspB1 in both RGC somas and axons after six weeks of injection (Supplementary Fig. S3B). The injection of AAV2-control did not result in the alteration of HspB1 in RGCs. Retinal flat mounts immunostained for Brn3a showed that only 57% of RGCs survived in MB injected eyes relative to the contralateral eyes (Figs. 2C, 2D; $P < 0.0001$). The AAV2-control injected eyes had 63% surviving RGCs compared to the control ($P < 0.001$); this was not statistically significant when compared to the vehicle control. However, AAV2-*HSPB1* treatment at 1 × 10^9 vg and 5 × 10^9 vg/retina robustly protected the RGCs; the surviving RGCs were 87% and 99% compared to the control, respectively. When compared to the vehicle

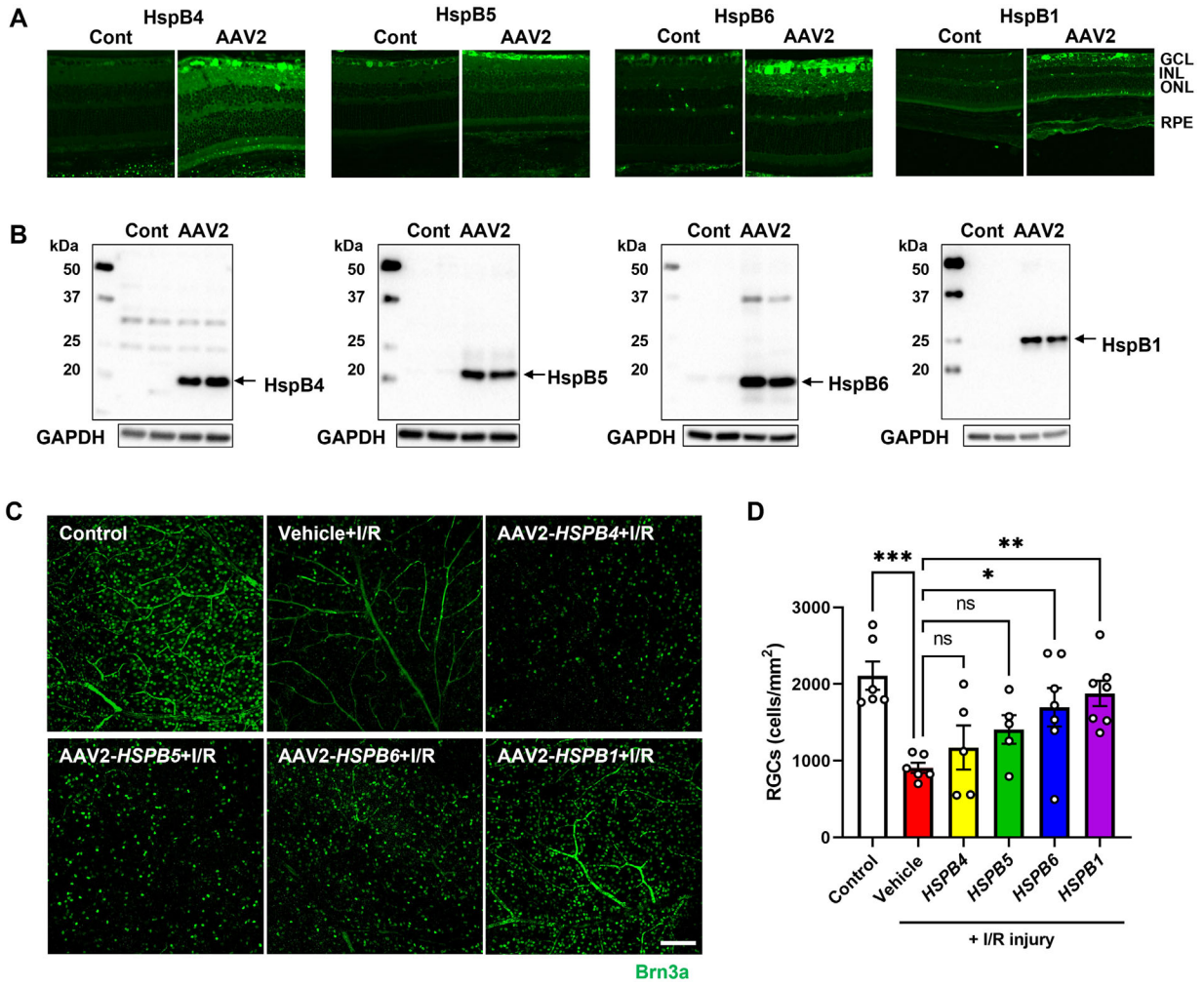

Figure 1. AAV2-sHsp protects RGCs from ischemia/reperfusion injury in mice. (A) Expression of sHsps in RGCs after AAV2-mediated delivery. AAV2-sHsps (1 µL from the stock of 1×10^{12} viral genomes/mL) were intravitreally injected into the right eye. The left eye was uninjected and served as the control. After four weeks, retinal sections were fixed and stained with antibodies to determine the expression of sHsps in the RGCs (N = 3). Magnification × 40. Cont, control; AAV-2, AAV2-sHsp-injected specimens. (B) After four weeks, whole retinas were homogenized. The homogenate was subjected to Western blotting for sHsp. In each Western blot, lanes 2 and 3 are controls, and lanes 4 and 5 are AAV2-sHsp-injected specimens. GAPDH was used as the loading control (N = 2). (C) Mice were subjected to I/R injury four weeks after intravitreal injection of AAV2-sHsp. Retinas were isolated, fixed and immunostained for RGCs with Brn3a antibody two weeks later. *Scale bar:* 100 µm. (D) The bar graph shows the number of RGCs/mm^2 in the mid-peripheral retina. Data represent the mean ± SEM for groups of five to seven mice. *$P < 0.05$; **$P < 0.01$; ***$P < 0.001$; ns, not significant; GCL, ganglion cell layer; INL, inner nuclear layer; ONL, outer nuclear layer; RPE, retinal pigment epithelium.

control, the RGC numbers were significantly higher in both 1×10^9 vg/retina ($P < 0.05$) and 5×10^9 vg/retina ($P < 0.01$) treated eyes. Brn3a labels about ~80% of the total RGCs in rodent retinas, and its expression could be decreased under stress conditions in surviving RGCs. [52] To determine whether Brn3a labeling accurately reflected RGC death, we verified the effect of AAV2-*HSPB1* on RGCs by RBPMS labeling. RPBMS staining showed 67% ($p < 0.001$) and 92% surviving RGCs in the AAV2-control and AAV2-*HSPB1* (1×10^9 vg/retina) injected eyes compared to the controls, respectively (Supplementary Fig. S4). Together, these data suggested that the overexpression of HspB1 prevented the loss of RGCs after IOP elevation.

We next measured anterograde transport to assess RGC axonal health. The fluorescence intensity from intravitreally injected cholera toxin subunit B conjugated to Alexa Fluor 555 (CT-B) was measured from along the length of the optic nerve up to the optic chiasm, as previously described. [53] In control animals, CT-B fluorescence was present throughout the length

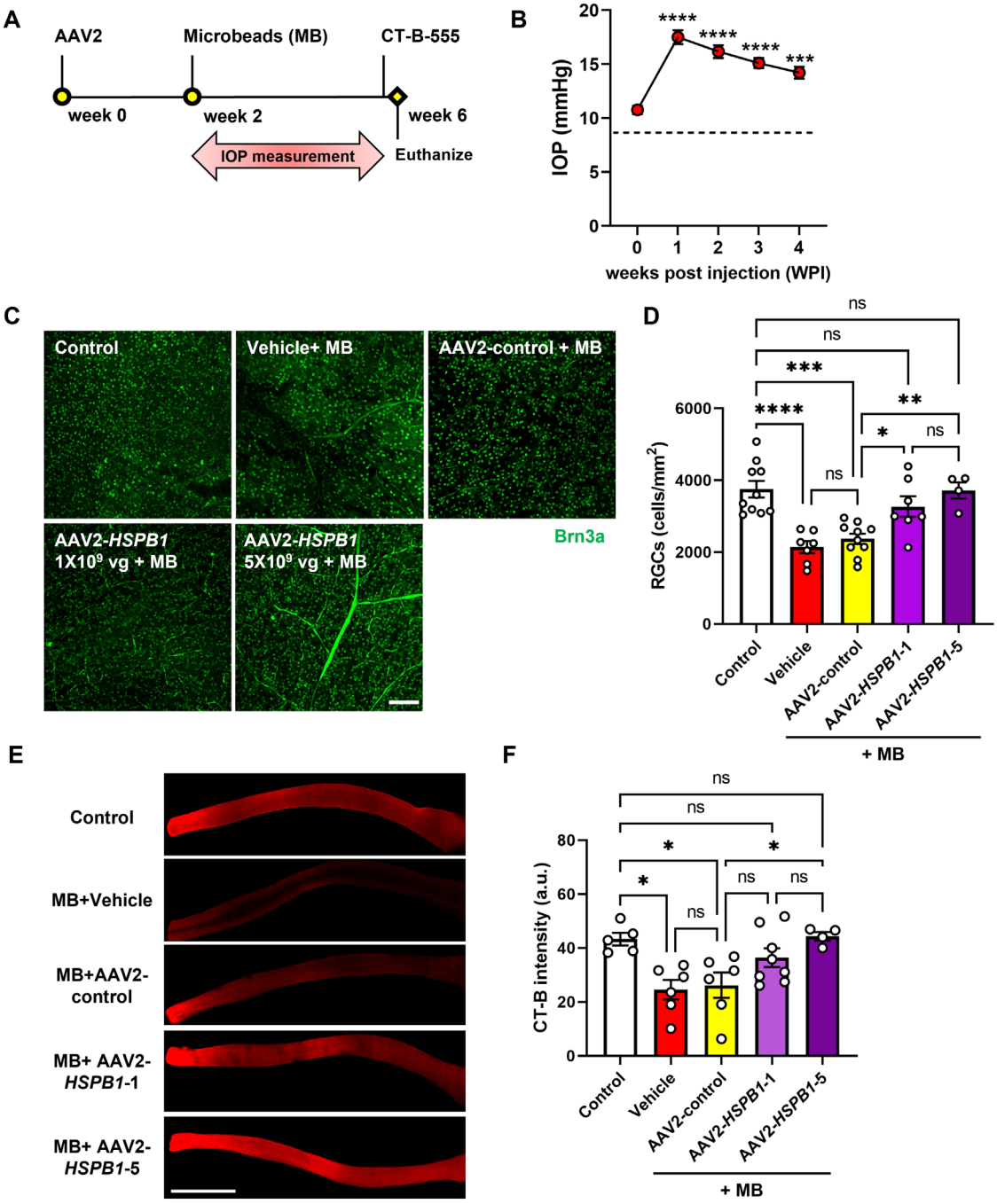

Figure 2. Prophylactic effects of AAV2-*HSPB1* in a mouse model of glaucoma. (A) The AAV2-*HSPB1* injection timeline for a mouse model of glaucoma is shown. MBs were injected into the anterior chamber of one eye two weeks after the intravitreal injection of AAV2-*HSPB1* (1 µL from the stock of 1×10^{12} viral genomes/mL and 2 µL from the stock of 2.5×10^{12} viral genomes/mL). Four weeks later, retinal flatmounts were fixed and immunostained for RGCs. (B) The IOP of MB-injected eyes was significantly elevated one week post-MB injection (WPI). (C) After immunostaining whole retinal flatmounts with Brn3a, four areas in the mid-periphery were selected to determine RGC density. Confocal microscopic images were captured from the selected retinal areas in the contralateral (control), vehicle-treated, AAV2-control-treated, and AAV2-*HSPB1*-treated groups at four WPI. *Scale bar:* 100 µm. (D) The bar graph shows the number of RGCs. (E) Mice were injected as above, and after four weeks, Alexa Fluor 555-conjugated CT-B (1 µL, 0.2%) was injected intravitreally. The animals were killed 24 hours after CT-B injection and the optic nerves were dissected out. Confocal microscopic (TRITC filter) images were captured along the length of the optic nerve. *Scale bar:* 1000 µm. (F) Quantification of the CT-B intensity. Data represent the mean ± SEM of four to eight independent experiments. Each data point represents one animal. $^{*}P < 0.05$; $^{**}P < 0.01$; $^{***}P < 0.001$; $^{****}P < 0.0001$. ns, not significant.

of the optic nerve (Figs. 2E, 2F). Four weeks after MB injection, the CT-B intensity significantly ($P < 0.05$) decreased by 43% compared to the control. The administration of AAV2-control also showed a 39% decrease, which was not significant when compared to vehicle-treated eyes ($P < 0.05$). However, on AAV2-*HSPB1* administration, the CT-B labeling intensity was 84% of that of the control at a viral load of 1×10^9 vg/retina. Interestingly, the CT-B fluorescence intensity with the injection of a viral load of 5×10^9 vg/retina showed the same level as the control group, indicating that HspB1 expression before the injury successfully prevented the ocular hypertension-mediated axonal transport deficits. However, because there were no significant differences between 1×10^9 and 5×10^9 vg/retina in RGC survival and functionality, we tested the protective ability of AAV2-*HSPB1* at the lower concentration in subsequent experiments.

Therapeutic Effects of AAV2-*HSPB1* in a Mouse Model of Glaucoma

We tested whether AAV2-*HSPB1* protects RGCs in mice with established ocular hypertension. AAV2-*HSPB1* was injected into the vitreous one week after MB injection (Fig. 3A). To maintain high IOP levels, we injected MB a second time three weeks after the

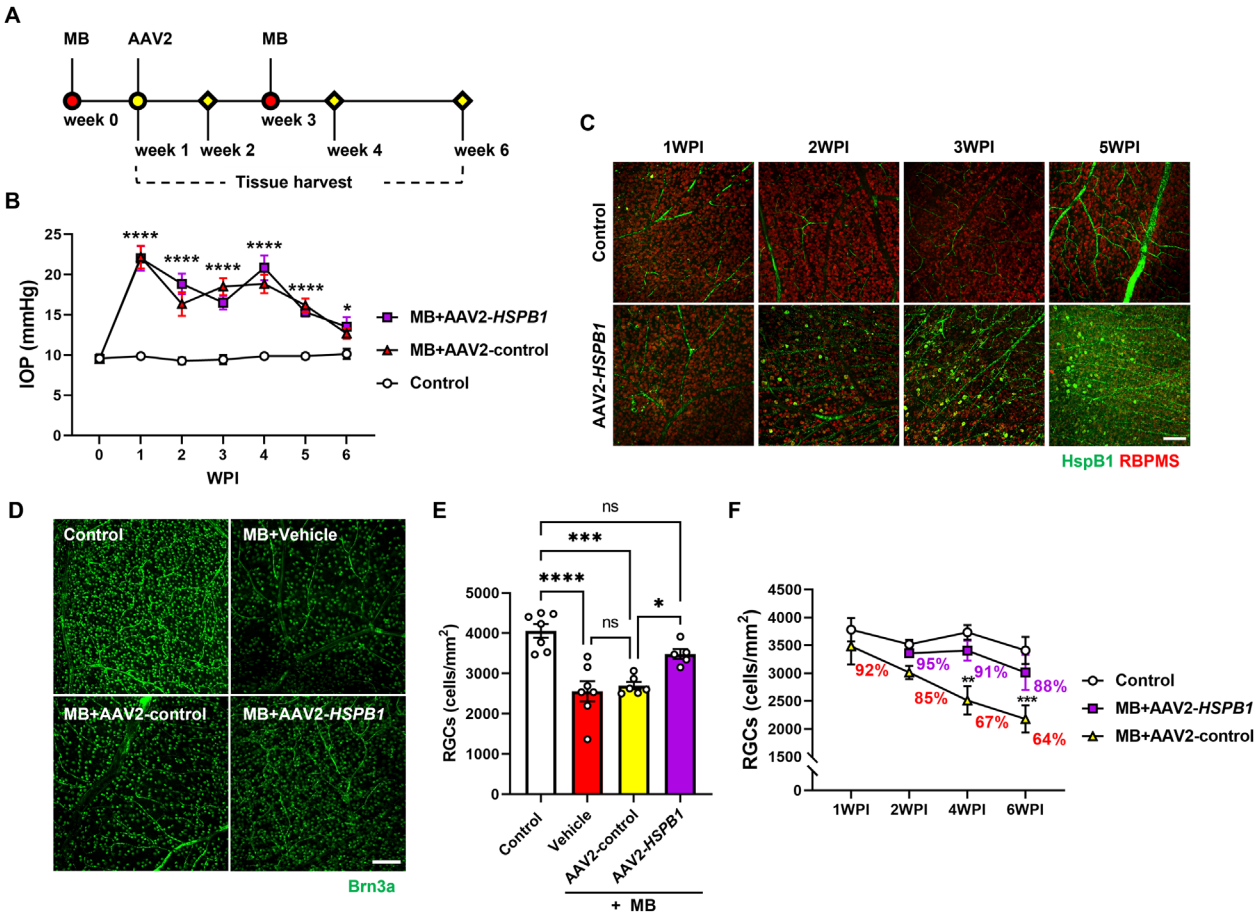

Figure 3. Therapeutic effects of AAV2-*HSPB1* in a mouse model of glaucoma: Effect on the time-dependent progression of RGC death. (A) The AAV2-*HSPB1* injection timeline for a mouse model of glaucoma is shown. MB were injected into the anterior chamber of one eye one week before the AAV2-*HSPB1* injection (1 µL from the stock of 1×10^{12} viral genomes/mL). Five weeks later, retinal flat mounts were fixed and immunostained for RGCs and HspB1. (B) The IOP of MB-injected eyes was significantly elevated at one WPI and remained significantly higher for six weeks. (C) Retinal flat mounts were immunostained for HspB1 and RPBMS (for RGCs). AAV2-*HSPB1* injection resulted in robust expression of HspB1 in RGCs at 5 WPI. (D) The Brn3a +ve RGCs from the mid-peripheral retina are shown for each group. Confocal microscopic images were captured in contralateral (control), MB + vehicle-treated, MB + AAV2-control-treated, and MB + AAV2-*HSPB1*-treated groups at six WPI. (E) The bar graph shows the quantification of Brn3a +ve RGC loss in retinal flat mounts. Data represent the mean ± SEM of 5-7 independent experiments. Each data point represents one animal. (F) Effect of AAV2-*HSPB1* treatment on the time-dependent RGC loss in the mid-peripheral retina one, two, four, and six WPI is shown. *$P < 0.05$; **$P < 0.01$; ***$p < 0.001$; ****$P < 0.0001$. ns, not significant. *Scale bar:* 100 µm.

first injection. The MB injection significantly elevated IOP ($P < 0.0001$) after one week, and the elevation was sustained over six weeks (Fig. 3B). There was no difference in the IOP levels between AAV2-*HSPB1*- and AAV2-control-injected eyes. To determine the optimum time window for the maximum expression of HspB1, we immunostained retinal flat mounts (from retinas harvested at one-week intervals) for HspB1. HspB1 expression in RGC somas was detectable at one-week after AAV2-*HSPB1* injection; the expression gradually increased over a five-week postinjection period (Fig. 3C). HspB1 was detectable in RGC somas and axons after three weeks, and the levels increased at five weeks after injection. Six weeks after MB injection, RGC numbers were significantly decreased in the vehicle (37%, $P < 0.0001$) and AAV2-control-treated (33%, $P < 0.001$) groups when compared to the control (Fig. 3D, 3E). In contrast, the intravitreal delivery of AAV2-*HSPB1* significantly ($P < 0.05$) inhibited RGC loss; the remaining RGCs were 86% of the controls. These results indicated that AAV2-*HSPB1* may halt RGC death after injury onset.

We next determined whether a single administration of AAV2-*HSPB1* can stop RGC loss in IOP-elevated eyes when RGC loss has already begun. This situation is relevant to the clinical setting, where glaucoma patients often have lost some degree of vision because of RGC loss at their first visit. AAV2-*HSPB1* was injected into the vitreous one week after MB injection; mice were killed at one, two, four, and six weeks after MB injection. Control eyes did not show changes in RGC number. However, the RGC numbers in the AAV2-control-injected eyes were approximately 92% of the control eyes at one week after MB injection, and they were 85%, 67%, and 64% at two, four, and six weeks after MB injection, respectively (Fig. 3F). In the eyes that received AAV2-*HSPB1* one week after MB injection, the surviving RGCs were 95%, 91%, and 88% at two, four, and six weeks after MB injection, respectively. Representative retinal images are shown in Supplementary Figure S5. These results suggested that a single injection of AAV2-*HSPB1* protected RGCs despite a sustained elevation in IOP and that the protection of RGCs was consistently significant over six weeks.

Next, we determined whether treatment with AAV2-*HSPB1* in IOP-elevated eyes prevented anterograde axon transport deficits. After six weeks of IOP elevation, the fluorescence intensity of CT-B in the optic nerve was decreased by 22% and 32% in the vehicle and AAV2-control-injected groups, respectively (Fig. 4A and 4B). However, the administration of AAV2-*HSPB1* significantly ($P < 0.05$) protected the reduction in CT-B intensity; the decrease was only 8% compared to the control. Together, these results suggested that AAV2-*HSPB1* gene therapy in IOP-elevated eyes simultaneously inhibited somal and axonal damage in RGCs.

Several studies have shown that excessive microglial activation can cause synapse loss and contribute to the death of RGCs in glaucoma.[54] In addition, astrocytes and Müller glia, which provide stability to neural tissue under normal conditions, show abnormal activity in response to damage, resulting in the upregulation of GFAP, which can interfere with axonal transport in glaucoma.[55] Therefore we assessed the effect of AAV2-*HSPB1* on glial activation in ocular hypertension. MB-mediated IOP elevation caused microglial activation after one week, and it gradually increased over the remaining period of the experiment (Supplementary Fig. S6). Six weeks after MB injection, microglial cells were highly activated, but the AAV2-*HSPB1*–injected group showed decreased activated microglial cells compared to the AAV2-control-injected group (Fig. 4C). Immunostaining for GFAP was robustly increased in the MB-injected AAV2-control group, but it was reduced in the AAV2-*HSPB1*–injected group (Fig. 4D). These results suggested that RGC-specific HspB1 expression inhibited retinal glial activation.

Long-Term Study

We then assessed the long-term protective effects of AAV2-*HSPB1*. We injected MB at the start of the study and at three and six weeks after the first injection to maintain elevated IOP. The IOP was elevated in a sustained manner up to 10 weeks and slowly decreased over the next 10 weeks (Figs. 5A, 5B). As shown in Figures 5C and 5D, the elevation of IOP led to a decrease in the number of RGCs by 50% ($P < 0.0001$) at 20 weeks after MB injection when compared to the control, whereas one-time injection of AAV2-*HSPB1* significantly inhibited RGC loss; the remaining RGCs were 84% of the control, and it was significantly ($P < 0.0001$) higher than AAV2-control-injected group. In addition to RGC survival, we also assessed the function of RGCs. The pERG waveform and the P1 amplitude showed reduced signals by 38% in the MB+AAV2-control group when compared to the uninjected control group ($P < 0.01$). The injection of AAV2-*HSPB1* significantly ($P < 0.05$) inhibited the IOP-mediated pERG amplitude reduction; the reduction was only 9% when compared to the control eyes (Figs. 5E, 5F). These results indicated that intravitreal delivery of AAV2-*HSPB1* had sustained beneficial effects on RGCs over the study period.

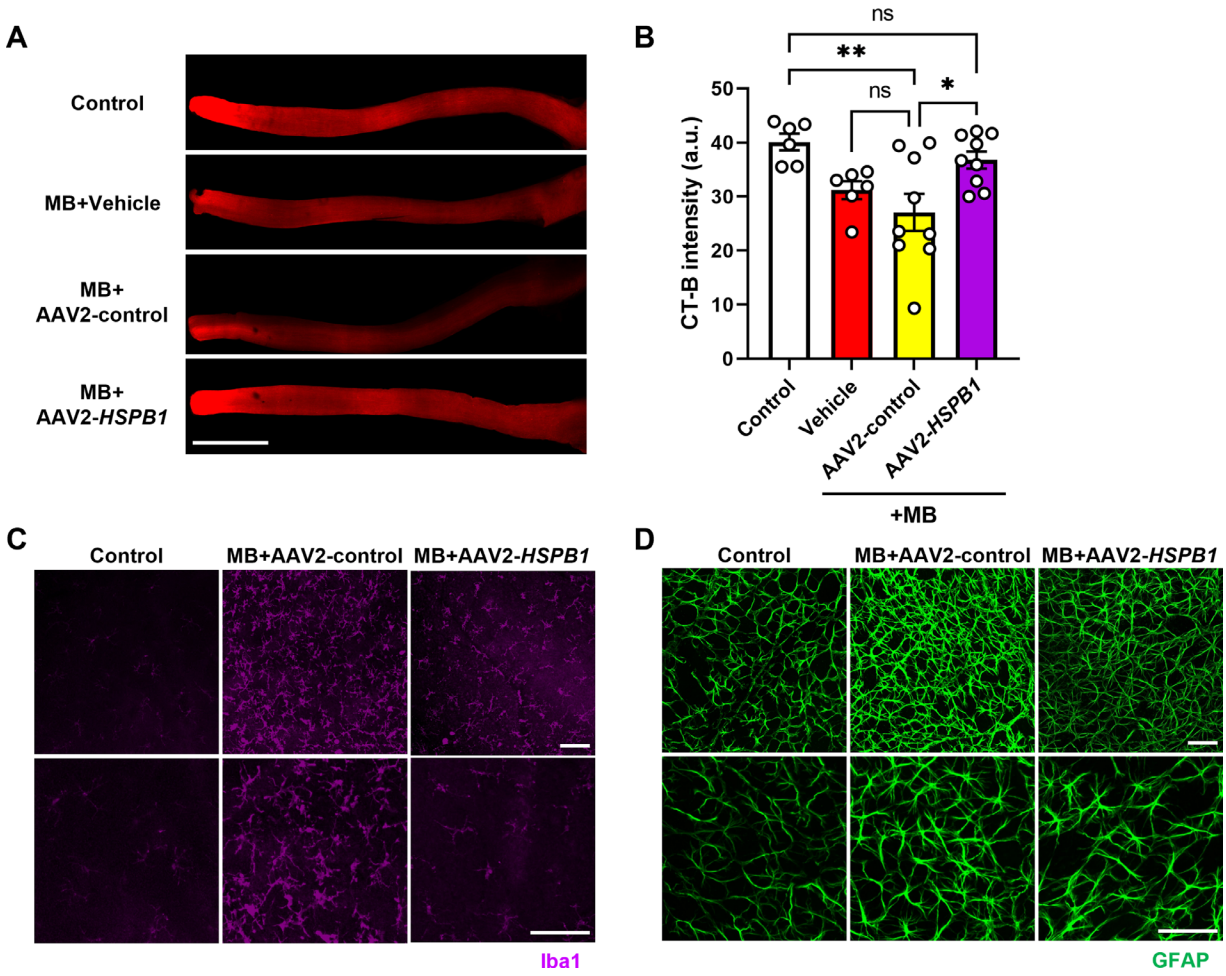

Figure 4. Therapeutic effects of AAV2-*HSPB1* in a mouse model of glaucoma: Effects on axonal transport and glial activation. MB were injected into the anterior chamber of the eye one week before and two weeks after AAV2-control or AAV2-*HSPB1* injection. (A) Six weeks after MB injection, mice were intravitreally injected with Alexa Fluor 555-conjugated CT-B (1 µL, 0.2%), and the optic nerve was isolated. Confocal microscopic images were captured along the entire length of the optic nerve. *Scale bar:* 1000 µm. (B) Quantification of the CT-B intensity. (C, D) Inhibitory effect of AAV2-*HSPB1* on glial activation. Six weeks after MB injection, representative images of the retinal GCL layer showing (C) Iba1 (activated microglial marker, purple) and (D) GFAP (activated astrocyte marker, green) in retinal flat mounts. Data represent the mean ± SEM of six to nine (A, B) and three to four (C, D) independent experiments. Each data point represents one animal. *$P < 0.05$; **$P < 0.01$. ns, not significant. *Scale bar:* 100 µm.

Discussion

The objectives of this study were to determine which of the four tested sHsps was better at protecting RGCs under glaucomatous stress and to determine whether the RGC-specific expression of sHsps prevents somal and axonal damage in a mouse model of glaucoma. We found that HspB1 is better than the other three in preventing RGC death under I/R stress.

Notably, several previous studies have shown that HspB1 levels in the retinas of animal models of glaucoma are elevated when RGC numbers are decreased. For example, one study showed that intravitreal injection of HspB1 caused degeneration of RGCs in rat retinas.[35] Other studies have shown that HspB1 levels are elevated in an experimental rat model of glaucoma[56,57] and in rat eyes subjected to an acute elevation of IOP after 30-90 minutes.[58] These studies suggested that elevated HspB1 or exogenous HspB1 supplementation is harmful to RGCs. However, other studies indicated that high levels of HspB1 protected RGCs under conditions that promote their death. For example, HspB1 upregulation through cobalt chloride administration protected rat retinal RGCs when subjected to ischemic injury.[59] The induction of HspB1 and protection of RGCs were observed after intravitreal injection of the HMG-

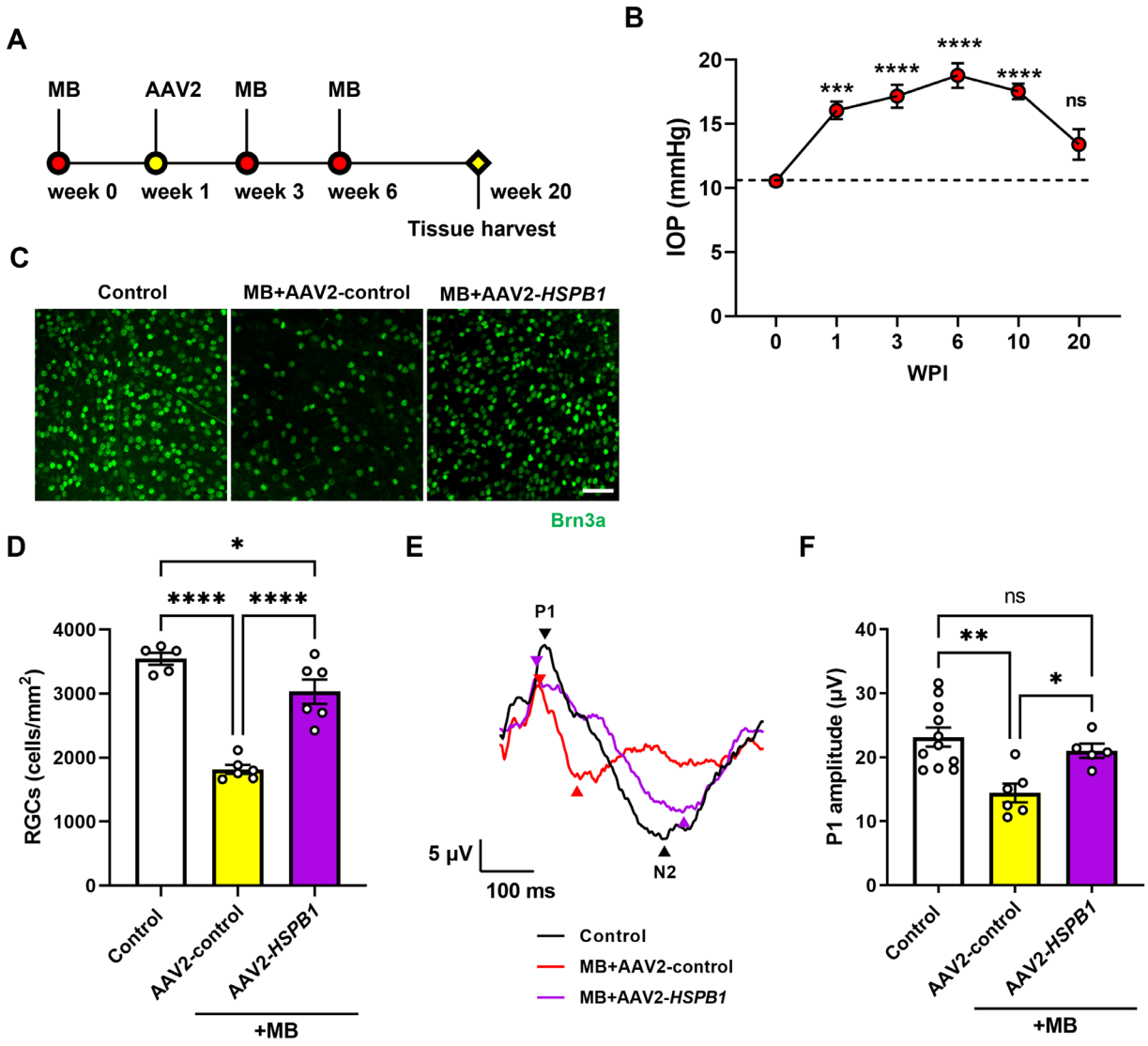

Figure 5. Long-term efficacy of AAV2-*HSPB1* in a mouse model of glaucoma: Effects on axonal transport and glial activation. (A) The AAV2-*HSPB1* injection timeline for a mouse model of glaucoma is shown. MB were injected into the anterior chamber of the eye at the start of the experiment and at three weeks and six weeks. AAV2-control or AAV2-*HSPB1* (1 µL from the stock of 1×10^{12} viral genomes/mL) was injected intravitreally one WPI. (B) The IOP of MB-injected eyes was significantly elevated one WPI, remained significantly higher over ten weeks and then gradually decreased between 10-20 weeks. (C) After 20 weeks, retinas were isolated, retinal flat mounts were fixed and immunostained for RGCs (Brn3a, green). Confocal microscopic images were captured from the mid-peripheral regions of the retina in the contralateral (control), MB + AAV2-control-treated, and MB + AAV2-*HSPB1*-treated groups at 20 weeks. (D) Bar graph showing Brn3a +ve RGCs in retinal flat mounts. (E) Representative pERG response at 20 weeks. (F) Quantification of the P1 amplitude of pERG. Data represent the mean ± SEM of five to 11 independent experiments. Each data point represents one animal. *$P < 0.05$; **$P < 0.01$; ***$P < 0.001$; ****$P < 0.0001$; ns = not significant. *Scale bar:* 50 µm.

CoA reductase inhibitor simvastatin after optic nerve axotomy.[60] Furthermore, ischemia-mediated preconditioning caused an increase in the expression of HspB1, which protected RGCs after optic nerve injury in rats.[61] Similar beneficial effects of HspB1 were observed in I/R-injured mouse retinas.[34] These seemingly contrasting effects of HspB1 are puzzling. One likely explanation for the conundrum is that the elevation of HspB1 in some of the animal models mentioned above may not occur within RGCs but may occur in other cells of the retina; hence, the lack of RGC protection. Another point to be noted here is that studies that used recombinant HspB1 might have inadvertently introduced minor contaminants (present in the protein preparation) into the eye. Bacterial-expressed sHsps invariably have minor proteins that copurify with sHsps (possi-

bly because of their binding to sHsps), which could have caused RGC death. Further studies are needed to clarify this issue.

Another possibility to consider is that HspB1, even though upregulated in animal models of glaucoma, could become less active or inactive because of posttranslational modifications and consequently less able to protect RGCs. Although phosphorylation is likely to enhance its activity,[62] other modifications, if co-occurring, could have the opposite effect. Support for this notion comes from studies on HspB5 in animal models of diabetic retinopathy, where HspB5 is upregulated,[63] but its chaperone activity is compromised, likely because of posttranslational modifications.[64]

Another issue is related to autoantibodies against HspB1. RGC death and axonal degeneration have been noted in rats immunized with HspB1 followed by elevation of IOP.[65] Furthermore, serum autoantibodies for HspB1 are elevated in glaucoma patients,[66] and such autoantibodies have been shown to cause RGC death.[67] The eyes are somewhat immune privileged; therefore exogenous HspB1 in the eye may not elicit an immune response. In our study, the possibility of an immune response is even less likely, as we expressed HspB1 only in RGCs. Such expression did not affect the morphology of retina or other eye tissues after six weeks of AAV2-*HSPB1* injection.

We envision several mechanisms by which HspB1 protects RGCs: (1) HspB1 is a stress-inducible molecular chaperone. Under normal conditions, HspB1 exists as large oligomers with a molecular mass up to 800 kDa.[68] Nevertheless, under stress conditions, HspB1 is phosphorylated and assumes a smaller dimeric and oligomeric structure, which enhances its chaperone activity.[69] Through its ATP-independent chaperone activity, it binds partially denatured proteins, preventing them from undergoing complete denaturation and loss of their activity. Whether the expression of HspB1 in RGCs prevents protein denaturation and thereby protects against RGC death needs further investigation. (2) Another mechanism is related to the antiapoptotic activity of HspB1. HspB1 inhibits apoptosis through interactions with key components of the apoptotic signaling pathway; it inhibits Bax-mediated mitochondrial apoptosis through activation of the cell survival PI3-kinase/AKT pathway.[70] In addition, HsPB1 can bind to cytochrome c and procaspase-3 and bind to tumor necrosis factor–related apoptosis-inducing ligand and Fas, all of which can inhibit apoptosis.[71,72] (3) The ability of HspB1 to prevent oxidative damage through upregulation of cellular GSH and reduction of ROS[73,74] is yet another possible mechanism by which it can prevent RGC death in IOP-elevated eyes. A previous study reported that in the mouse eye subjected to optic nerve crush, among the 40+ subtypes of RGCs, some were resistant, whereas others were susceptible to death.[53] It is possible that HspB1 expression prevented the death of ocular hypertension susceptible RGCs.

In our study, the expression of HspB1 in RGCs attenuated IOP-induced anterograde axonal transport defects. HspB1 plays a key role in preventing cytoskeletal protein damage in stressed cells.[75–78] In glaucoma, the disruption of axonal cytoskeletal proteins, such as neurofilaments, microtubules, and tau, has been observed.[79] Tau, a neuronal microtubule-associated protein, plays a crucial role in the maintenance and function of axons. In glaucoma, tau assembles into abnormal filaments via hyperphosphorylation, impairs axonal transport, and increases susceptibility to excitotoxic damage.[80] Previous studies have shown that HspB1 directly binds to hyperphosphorylated tau and degrades it[81,82]; thus HspB1-mediated microtubule stabilization likely improves the axonal transport rate.

Microglia and astrocytes, immunocompetent cells of the central nervous system, have important roles in initiating the inflammatory process and tissue repair in the retina.[83] Microglia and astrocytes are mainly located in the ganglion cell layer. When activated, they release inflammatory mediators such as cytokines, reactive oxygen species, and tumor necrosis factor–α, leading to inflammatory damage.[84] We observed that microglial activation was attenuated by AAV2-*HSPB1* in our mouse model of glaucoma, which could have played a role in the prevention of RGC death.

There was a disconnect between RGC loss and P1 amplitude reduction in the MB injected eyes; whereas the loss of RGCs was ~50% after 20 weeks of MB injection, the reduction in P1 amplitude was ~38%. Although the general consensus is that the pERG response is a well-accepted indicator of RGC function in early glaucoma, pERG amplitude and the RGC counts are not expected to be perfectly linear in magnitude over time. Whether AAV2-*HSPB1* injection inhibits axonal damage needs to be investigated. Another point to note is that AAV2-*HSPB6* injection showed RGC protection comparable to AAV2-*HSPB1* during the I/R injury. Further studies are needed to determine its efficacy in animal models of glaucoma.

In conclusion, intravitreal administration of AAV2-*HSPB1* showed RGC-specific expression of HspB1, which protected both RGC somas and axons in mouse eyes with elevated IOP. The ability to protect RGCs in a sustained manner with a single intravitreal administration of AAV2-*HSPB1* has attractive potential for development as adjunctive gene therapy (in addition to IOP-lowering therapies) to save vision in glaucoma.

Acknowledgments

The authors thank Dorota Stankowska, Johanna Rankenberg and Sudipta Panja for critical reading of the manuscript.

Supported by a SPARK/REACH grant (DO-2021-2472) and an RPB unrestricted grant to the Department of Ophthalmology, University of Colorado School of Medicine.

Disclosure: **M.-H. Nam**, None; **R.B. Nahomi**, None; **M.B. Pantcheva**, None; **A. Dhillon**, None; **V.A. Chiodo**, None; **W.C. Smith**, None; **R.H. Nagaraj**, None

References

1. Allison K, Patel D, Alabi O. Epidemiology of glaucoma: The past, present, and predictions for the future. *Cureus*. 2020;24:e11686.
2. John SW. Mechanistic insights into glaucoma provided by experimental genetics the cogan lecture. *Invest Ophthalmol Vis Sci*. 2005;46:2649–2661.
3. Gupta SK, Niranjan DG, Agrawal SS, Srivastava S, Saxena R. Recent advances in pharmacotherapy of glaucoma. *Indian J Pharmacol*. 2008;40:197–208.
4. Ang A, Reddy MA, Shepstone L, Broadway DC. Long term effect of latanoprost on intraocular pressure in normal tension glaucoma. *Br J Ophthalmol*. 2004;88:630–634.
5. Almasieh M, Wilson AM, Morquette B, Cueva Vargas JL, Di Polo A. The molecular basis of retinal ganglion cell death in glaucoma. *Prog Retin Eye Res*. 2012;31:152–181.
6. Munemasa Y, Kitaoka Y. Molecular mechanisms of retinal ganglion cell degeneration in glaucoma and future prospects for cell body and axonal protection. *Front Cell Neurosci*. 2012;6:60.
7. Howell GR, Soto I, Libby RT, John SW. Intrinsic axonal degeneration pathways are critical for glaucomatous damage. *Exp Neurol*. 2013;246:54–61.
8. Mittag T, Schmidt KG. Mechanisms of neuroprotection against glaucoma. *Ophthalmologe*. 2004;101:1076–1086.
9. Jiang C, Moore MJ, Zhang X, Klassen H, Langer R, Young M. Intravitreal injections of GDNF-loaded biodegradable microspheres are neuroprotective in a rat model of glaucoma. *Mol Vis*. 2007;13:1783–1792.
10. Lambert WS, Ruiz L, Crish SD, Wheeler LA, Calkins DJ. Brimonidine prevents axonal and somatic degeneration of retinal ganglion cell neurons. *Mol Neurodegener*. 2011;6:4.
11. Anders F, Teister J, Liu A, et al. Intravitreal injection of beta-crystallin B2 improves retinal ganglion cell survival in an experimental animal model of glaucoma. *PLoS One*. 2017;12:e0175451.
12. Teister J, Anders F, Beck S, et al. Decelerated neurodegeneration after intravitreal injection of alpha-synuclein antibodies in a glaucoma animal model. *Sci Rep*. 2017;7:6260.
13. Pitha I, Kimball EC, Oglesby EN, et al. Sustained Dorzolamide Release Prevents Axonal and Retinal Ganglion Cell Loss in a Rat Model of IOP-Glaucoma. *Transl Vis Sci Technol*. 2018;7:13.
14. Nagaraj RH, Nahomi RB, Mueller NH, Raghavan CT, Ammar DA, Petrash JM. Therapeutic potential of alpha-crystallin. *Biochim Biophys Acta*. 2016;1860:252–257.
15. Webster JM, Darling AL, Uversky VN, Blair LJ. Small Heat Shock Proteins, Big Impact on Protein Aggregation in Neurodegenerative Disease. *Front Pharmacol*. 2019;10:1047.
16. Schmidt T, Fischer D, Andreadaki A, Bartelt-Kirbach B, Golenhofen N. Induction and phosphorylation of the small heat shock proteins HspB1/Hsp25 and HspB5/alphaB-crystallin in the rat retina upon optic nerve injury. *Cell Stress Chaperones* .2016;21:167–178.
17. Lanneau D, Brunet M, Frisan E, Solary E, Fontenay M, Garrido C. Heat shock proteins: essential proteins for apoptosis regulation. *J Cell Mol Med*. 2008;12:743–761.
18. Erni ST, Fernandes G, Buri M, et al. Anti-inflammatory and oto-protective effect of the small heat shock protein alpha B-crystallin (HspB5) in experimental pneumococcal meningitis. *Front Neurol*. 2019;10:570.
19. Miller-Graziano CL, De A, Laudanski K, Herrmann T, Bandyopadhyay S. HSP27: an anti-inflammatory and immunomodulatory stress protein acting to dampen immune function. *Novartis Found Symp*. 2008;291:196–208; discussion 208-111, 221-194.
20. Manzanares D, Bauby C, de la Pena R, et al. Antioxidant properties of alpha-crystallin. *J Protein Chem*. 2001;20:181–189.
21. Stankowska DL, Nam MH, Nahomi RB, et al. Systemically administered peptain-1 inhibits retinal ganglion cell death in animal models: implications for neuroprotection in glaucoma. *Cell Death Discov*. 2019;5:112.
22. Piri N, Song M, Kwong JM, Caprioli J. Modulation of alpha and beta crystallin expression

in rat retinas with ocular hypertension-induced ganglion cell degeneration. *Brain Res*. 2007;1141: 1–9.
23. Piri N, Kwong JM, Caprioli J. Crystallins in retinal ganglion cell survival and regeneration. *Mol Neurobiol*. 2013;48:819–828.
24. Miyara N, Shinzato M, Yamashiro Y, Iwamatsu A, Kariya KI, Sawaguchi S. Proteomic analysis of rat retina in a steroid-induced ocular hypertension model: potential vulnerability to oxidative stress. *Jpn J Ophthalmol*. 2008;52:84–90.
25. Steele MR, Inman DM, Calkins DJ, Horner PJ, Vetter ML. Microarray analysis of retinal gene expression in the DBA/2J model of glaucoma. *Invest Ophthalmol Vis Sci*. 2006;47:977–985.
26. Thanos S, Bohm MR, Schallenberg M, Oellers P. Traumatology of the optic nerve and contribution of crystallins to axonal regeneration. *Cell Tissue Res*. 2012;349:49–69.
27. Anders F, Liu A, Mann C, et al. The small heat shock protein alpha-crystallin B shows neuroprotective properties in a glaucoma animal model. *Int J Mol Sci*. 2017;18:2418.
28. Wu N, Yu J, Chen S, et al. alpha-Crystallin protects RGC survival and inhibits microglial activation after optic nerve crush. *Life Sci*. 2014;94:17–23.
29. Munemasa Y, Kwong JM, Caprioli J, Piri N. The role of alphaA- and alphaB-crystallins in the survival of retinal ganglion cells after optic nerve axotomy. *Invest Ophthalmol Vis Sci*. 2009;50:3869–3875.
30. Kalesnykas G, Niittykoski M, Rantala J, et al. The expression of heat shock protein 27 in retinal ganglion and glial cells in a rat glaucoma model. *Neuroscience*. 2007;150:692–704.
31. Krueger-Naug AM, Emsley JG, Myers TL, Currie RW, Clarke DB. Injury to retinal ganglion cells induces expression of the small heat shock protein Hsp27 in the rat visual system. *Neuroscience*. 2002;110:653–665.
32. Hebb MO, Myers TL, Clarke DB. Enhanced expression of heat shock protein 27 is correlated with axonal regeneration in mature retinal ganglion cells. *Brain Res* . 2006;1073:146–150.
33. Li Y, Roth S, Laser M, Ma JX, Crosson CE. Retinal preconditioning and the induction of heat-shock protein 27. *Invest Ophthalmol Vis Sci*. 2003;44:1299–1304.
34. Yokoyama A, Oshitari T, Negishi H, Dezawa M, Mizota A, Adachi-Usami E. Protection of retinal ganglion cells from ischemia-reperfusion injury by electrically applied Hsp27. *Invest Ophthalmol Vis Sci*. 2001;42:3283–3286.
35. Grotegut P, Kuehn S, Dick HB, Joachim SC. Destructive effect of intravitreal heat shock protein 27 application on retinal ganglion cells and neurofilament. *Int J Mol Sci*. 2020;21: 549.
36. Grotegut P, Hoerdemann PJ, Reinehr S, Gupta N, Dick HB, Joachim SC. Heat shock protein 27 injection leads to caspase activation in the visual pathway and retinal T-cell response. *Int J Mol Sci*. 2021;22:513.
37. Chen H, Cho KS, Vu THK, et al. Commensal microflora-induced T cell responses mediate progressive neurodegeneration in glaucoma. *Nat Commun*. 2018;9:3209.
38. Hebb MO, Myers TL, Clarke DB. Enhanced expression of heat shock protein 27 is correlated with axonal regeneration in mature retinal ganglion cells. *Brain Res*. 2006;1073-1074:146–150.
39. Hickey DG, Edwards TL, Barnard AR, et al. Tropism of engineered and evolved recombinant AAV serotypes in the rd1 mouse and ex vivo primate retina. *Gene Ther*. 2017;24:787–800.
40. Wiley LA, Burnight ER, Kaalberg EE, et al. Assessment of adeno-associated virus serotype tropism in human retinal explants. *Hum Gene Ther*. 2018;29:424–436.
41. Lee SH, Yang JY, Madrakhimov S, Park HY, Park K, Park TK. Adeno-associated viral vector 2 and 9 transduction is enhanced in streptozotocin-induced diabetic mouse retina. *Mol Ther Methods Clin Dev*. 2019;13:55–66.
42. Ong T, Pennesi ME, Birch DG, Lam BL, Tsang SH. Adeno-associated viral gene therapy for inherited retinal disease. *Pharm Res*. 2019;36:34.
43. Simpson EM, Korecki AJ, Fornes O, et al. New MiniPromoter Ple345 (NEFL) drives strong and specific expression in retinal ganglion cells of mouse and primate retina. *Hum Gene Ther*. 2019;30:257–272.
44. Zolotukhin S, Potter M, Zolotukhin I, et al. Production and purification of serotype 1, 2, and 5 recombinant adeno-associated viral vectors. *Methods*. 2002;28:158–167.
45. Jacobson SG, Acland GM, Aguirre GD, et al. Safety of recombinant adeno-associated virus type 2-RPE65 vector delivered by ocular subretinal injection. *Mol Ther*. 2006;13:1074–1084.
46. Nam MH, Pantcheva MB, Rankenberg J, Nagaraj RH. Transforming growth factor-beta2-mediated mesenchymal transition in lens epithelial cells is repressed in the absence of RAGE. *Biochem J*. 2021;478:2285–2296.
47. Angelucci A, Clasca F, Sur M. Anterograde axonal tracing with the subunit B of cholera toxin: a

highly sensitive immunohistochemical protocol for revealing fine axonal morphology in adult and neonatal brains. *J Neurosci Methods*. 1996;65:101–112.
48. Porciatti V. Electrophysiological assessment of retinal ganglion cell function. *Exp Eye Res*. 2015;141:164–170.
49. Calkins DJ. Critical pathogenic events underlying progression of neurodegeneration in glaucoma. *Prog Retin Eye Res*. 2012;31:702–719.
50. Weinreb RN, Leung CK, Crowston JG, et al. Primary open-angle glaucoma. *Nat Rev Dis Primers*. 2016;2:16067.
51. Ito YA, Belforte N, Cueva Vargas JL, Di Polo A. A magnetic microbead occlusion model to induce ocular hypertension-dependent glaucoma in mice. *J Vis Exp*. 2016;e53731.
52. Rodriguez AR, Muller LPD, Brecha NC. The RNA binding protein RBPMS is a selective marker of ganglion cells in the mammalian retina. *J Comp Neurol*. 2014;522:1411–1443.
53. Tran NM, Shekhar K, Whitney IE, et al. Single-Cell Profiles of Retinal Ganglion Cells Differing in Resilience to Injury Reveal Neuroprotective Genes. *Neuron*. 2019;104:1039–1055.e1012.
54. Ramirez AI, de Hoz R, Salobrar-Garcia E, et al. The Role of Microglia in Retinal Neurodegeneration: Alzheimer's Disease, Parkinson, and Glaucoma. *Front Aging Neurosci*. 2017;9:214.
55. Gallego BI, Salazar JJ, de Hoz R, et al. IOP induces upregulation of GFAP and MHC-II and microglia reactivity in mice retina contralateral to experimental glaucoma. *J Neuroinflammation*. 2012;9:92.
56. Chidlow G, Wood JP, Casson RJ. Expression of inducible heat shock proteins Hsp27 and Hsp70 in the visual pathway of rats subjected to various models of retinal ganglion cell injury. *PLoS One*. 2014;9:e114838.
57. Huang W, Fileta JB, Filippopoulos T, Ray A, Dobberfuhl A, Grosskreutz CL. Hsp27 phosphorylation in experimental glaucoma. *Invest Ophthalmol Vis Sci*. 2007;48:4129–4135.
58. Windisch BK, LeVatte TL, Archibald ML, Chauhan BC. Induction of heat shock proteins 27 and 72 in retinal ganglion cells after acute pressure-induced ischaemia. *Clin Exp Ophthalmol*. 2009;37:299–307.
59. Whitlock NA, Agarwal N, Ma JX, Crosson CE. Hsp27 upregulation by HIF-1 signaling offers protection against retinal ischemia in rats. *Invest Ophthalmol Vis Sci*. 2005;46:1092–1098.
60. Kretz A, Schmeer C, Tausch S, Isenmann S. Simvastatin promotes heat shock protein 27 expression and Akt activation in the rat retina and protects axotomized retinal ganglion cells in vivo. *Neurobiol Dis*. 2006;21:421–430.
61. Liu X, Liang JP, Sha O, Wang SJ, Li HG, Cho EYP. Protection of retinal ganglion cells against optic nerve injury by induction of ischemic preconditioning. *Int J Ophthalmol*. 2017;10:854–861.
62. Jovcevski B, Kelly MA, Rote AP, et al. Phosphomimics Destabilize Hsp27 Oligomeric Assemblies and Enhance Chaperone Activity. *Chemistry & Biology*. 2015;22:186–195.
63. Reddy VS, Raghu G, Reddy SS, Pasupulati AK, Suryanarayana P, Reddy GB. Response of Small Heat Shock Proteins in Diabetic Rat Retina. *Investigative Ophthalmology & Visual Science*. 2013;54:7674–7682.
64. Ito K, Kamei K, Iwamoto I, Inaguma Y, Nohara D, Kato K. Phosphorylation-induced change of the oligomerization state of alpha B-crystallin. *J Biol Chem*. 2001;276:5346–5352.
65. Wax MB, Tezel G, Yang J, et al. Induced autoimmunity to heat shock proteins elicits glaucomatous loss of retinal ganglion cell neurons via activated T-cell-derived fas-ligand. *J Neurosci*. 2008;28:12085–12096.
66. Tezel G, Seigel GM, Wax MB. Autoantibodies to small heat shock proteins in glaucoma. *Invest Ophthalmol Vis Sci*. 1998;39:2277–2287.
67. Zhao W, Dai L, Xi XT, Chen QB, An MX, Li Y. Sensitized heat shock protein 27 induces retinal ganglion cells apoptosis in rat glaucoma model. *Int J Ophthalmol*. 2020;13:525–534.
68. Zantema A, Verlaan-De Vries M, Maasdam D, Bol S, van der Eb A. Heat shock protein 27 and alpha B-crystallin can form a complex, which dissociates by heat shock. *J Biol Chem*. 1992;267:12936–12941.
69. Jovcevski B, Kelly MA, Rote AP, et al. Phosphomimics destabilize Hsp27 oligomeric assemblies and enhance chaperone activity. *Chem Biol*. 2015;22:186–195.
70. Havasi A, Li ZJ, Wang ZY, et al. Hsp27 inhibits Bax activation and apoptosis via a phosphatidylinositol 3-kinase-dependent mechanism. *J Biol Chem*. 2008;283:12305–12313.
71. Mehlen P, Preville X, Chareyron P, Briolay J, Klemenz R, Arrigo AP. Constitutive expression of human hsp27, Drosophila hsp27, or human alpha B-crystallin confers resistance to TNF- and oxidative stress-induced cytotoxicity in stably transfected murine L929 fibroblasts. *J Immunol*. 1995;154:363–374.
72. Kamradt MC, Lu M, Werner ME, et al. The small heat shock protein alpha B-crystallin is a novel inhibitor of TRAIL-induced apoptosis that sup-

presses the activation of caspase-3. *J Biol Chem*. 2005;280:11059–11066.
73. Arrigo AP, Virot S, Chaufour S, Firdaus W, Kretz-Remy C, Diaz-Latoud C. Hsp27 consolidates intracellular redox homeostasis by upholding glutathione in its reduced form and by decreasing iron intracellular levels. *Antioxid Redox Signal*. 2005;7:414–422.
74. Mehlen P, Hickey E, Weber LA, Arrigo AP. Large unphosphorylated aggregates as the active form of hsp27 which controls intracellular reactive oxygen species and glutathione levels and generates a protection against TNFalpha in NIH-3T3-ras cells. *Biochem Biophys Res Commun*. 1997;241:187–192.
75. Guay J, Lambert H, Gingras-Breton G, Lavoie JN, Huot J, Landry J. Regulation of actin filament dynamics by p38 map kinase-mediated phosphorylation of heat shock protein 27. *J Cell Sci*. 1997;110(Pt 3):357–368.
76. Huot J, Houle F, Spitz DR, Landry J. HSP27 phosphorylation-mediated resistance against actin fragmentation and cell death induced by oxidative stress. *Cancer Res*. 1996;56:273–279.
77. Williams KL, Rahimtula M, Mearow KM. Hsp27 and axonal growth in adult sensory neurons in vitro. *BMC Neurosci*. 2005;6:24.
78. Benndorf R, Hayess K, Ryazantsev S, Wieske M, Behlke J, Lutsch G. Phosphorylation and supramolecular organization of murine small heat shock protein HSP25 abolish its actin polymerization-inhibiting activity. *J Biol Chem*. 1994;269:20780–20784.
79. Chidlow G, Ebneter A, Wood JP, Casson RJ. The optic nerve head is the site of axonal transport disruption, axonal cytoskeleton damage and putative axonal regeneration failure in a rat model of glaucoma. *Acta Neuropathol*. 2011;121:737–751.
80. Bull ND, Guidi A, Goedert M, Martin KR, Spillantini MG. Reduced axonal transport and increased excitotoxic retinal ganglion cell degeneration in mice transgenic for human mutant P301S tau. *PLoS One*. 2012;7:e34724.
81. Shimura H, Miura-Shimura Y, Kosik KS. Binding of tau to heat shock protein 27 leads to decreased concentration of hyperphosphorylated tau and enhanced cell survival. *J Biol Chem*. 2004;279:17957–17962.
82. Freilich R, Betegon M, Tse E, et al. Competing protein-protein interactions regulate binding of Hsp27 to its client protein tau. *Nat Commun*. 2018;9:4563.
83. Reichenbach A, Bringmann A. Glia of the human retina. *Glia*. 2020;68:768–796.
84. Cuenca N, Fernandez-Sanchez L, Campello L, et al. Cellular responses following retinal injuries and therapeutic approaches for neurodegenerative diseases. *Prog Retin Eye Res*. 2014;43:17–75.